

Multi-strengthening-mechanisms in a novel titanium alloy with $(\text{TiHf})_5\text{Si}_3$ particle-reinforcement

Yan Du^{1*}, Jinwen Lu¹, Wei Zhang¹, Yusheng Zhang^{1, 2}

1. Northwest Institute for Nonferrous Metal Research, Xi'an 710016, China

2. Xi'an Rare Metal Materials Institute Co. Ltd., Xi'an 710016, China

*Corresponding author, E-mail address: tooru18@hotmail.com

Abstract

The microstructure and mechanical properties of Ti-2Si-2Nb-2Fe-1Hf-1Ta-1W alloy with $(\text{TiHf})_5\text{Si}_3$ particle-reinforcement and their underlying relations have been studied. Electron microscope observations and correlative statistical analysis have been made to analyze microstructure evolution with heat treatments. The $(\text{TiHf})_5\text{Si}_3$ particles with 800 nm in diameter were found uniformly distributed at α/β boundaries and triple junctions and turned out to be stable even after heat treatments at high temperature for a long period, inhibiting grain growth and dislocation motion. In addition, multi-strengthening-mechanisms including particle strengthening, solid-solution strengthening, grain boundary strengthening and dislocation strengthening have been discussed.

Key words: titanium alloy; microstructure; mechanical property; strengthening.

1. Introduction

Titanium and its alloys are widely used as an important class of engineering materials in aerospace, nuclear, chemical plants and biomaterials fields due to their high strength-to-weight ratio and good corrosion resistance [1, 2]. It is well known that stable Ti_5Si_3 phase with a complex P63 hexagonal structure possessing high melting point normally can be formed in high silicon-containing Ti alloys and therefore can act as reinforcement even at high temperature [3-5]. However, high volume fraction of Ti_5Si_3 phase may depress the plasticity of the Ti alloys at room temperature due to its brittleness. Thus, increasing needs of the Ti alloys with good performances invoke widespread investigations on the relationship between microstructure and properties of newly designed silicon-containing Ti alloys. Recently, Ti-Si-X alloys with β -stabilizing elements have been proposed and exhibited improved plasticity [6, 7]. Our previous work also proved that the comprehensive mechanical properties of silicon-containing Ti alloys could be improved by adding multiple alloying elements including Nb, Fe, Hf, Ta and W [8]. However, the relationship between microstructure and properties and the underlying strengthening mechanisms of these Ti alloys have not been investigated sufficiently.

In this study, a novel Ti-2Si-2Nb-2Fe-1Hf-1Ta-1W alloy noted as Ti alloy in the following has been fabricated as researching object to study the relation between microstructure and mechanical properties. Multi-strengthening-mechanisms of this novel Ti alloy were discussed based on electron microscopy and correlated statistical analysis.

2. Experimental

The Ti alloy was fabricated by arc-melting followed by hot forging and hot rolling at 980 °C and 820 °C, respectively. Details of the fabrication processing, dimension and composition for this Ti alloy were given in our previous work [8]. Solution treatments were carried out at 800 °C and 900 °C, which are about 50 °C below and above β transus temperature of 847 °C, respectively, for 40 min followed by air cooling. Then, aging treatments were carried out at 500 °C for 6 h followed by air cooling for both solution conditions. Samples were kept for each condition including as-rolled Ti alloy before heat treatment, i.e. five types of samples denoted as as-rolled, 800 °C, 800 °C+500 °C, 900 °C and 900 °C+500 °C.

Microstructural characterizations were performed by using a scanning electron microscope (SEM, JEOL JSM-6700) and a transmission electron microscope (TEM, JEOL JEM-2100). For the SEM observations, samples were mechanically polished and etched by using a solution of HF:HNO₃:H₂O = 1:3:5 in volume. For the TEM observations, thin film samples were electropolished by twin-jet technique in a solution of 10 vol.% perchloric acid and 90 vol.% methanol at a voltage of 50 V with liquid nitrogen. Tensile tests were carried out on an Instron598X universal testing machine at a strain rate of 10⁻³ s⁻¹ at ambient temperature. Standard cylindrical tensile specimens with a gauge length of 25 mm and a gauge diameter of 5 mm were prepared and two specimens for each condition were tested.

3. Results

3.1 Microstructure

The overall microstructure of as-rolled sample is shown in Figure 1(a), showing fine equiaxed grains with uniform distribution of particle reinforcements. Figure 1(b) reveals a closer observation with high magnification on the microstructure, showing that the as-rolled Ti alloy consists of fine equiaxed α and β grains and particles distributed mostly at grain boundaries and triple junctions with an average diameter of 0.8 μm .

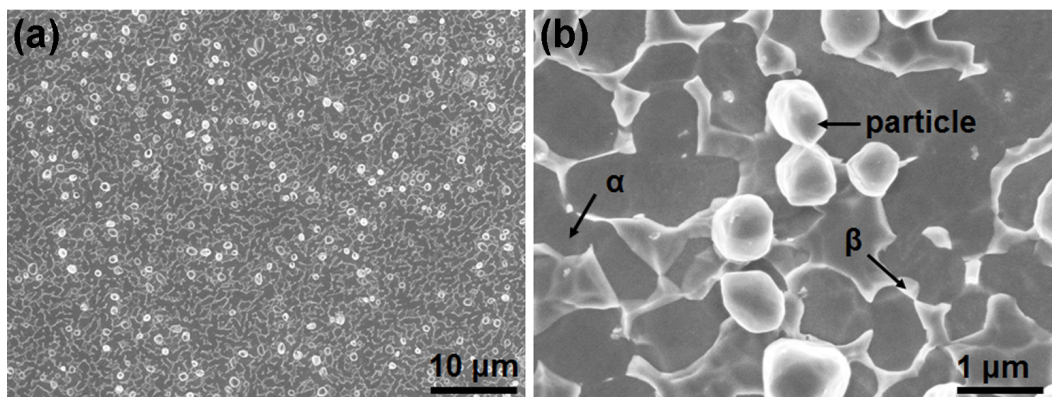


Figure 1. SEM observations of as-rolled Ti alloy: (a) overall microstructure; (b) high magnification showing microstructure consisting of particles, α and β phases.

The microstructures of the Ti alloys after different heat treatments are shown in Figure 2, showing that the average size of the particles does not change much with a slight growth to 1 μm . Figure 2(a) shows that after solution treatment at 800 °C, the Ti matrix consists of equiaxed α grains and $\beta+\alpha$ colonies with thin α lath. After aging treatment at 500 °C, the Ti matrix retains equiaxed α grains and $\beta+\alpha$ colonies with growth of α lath as shown in Figure 2(b). Figure 2(c) shows that after solution treatment at 900 °C, the Ti matrix consists of $\beta+\alpha$ colonies. After aging treatment at 500 °C, the Ti matrix retains $\beta+\alpha$ colonies with growth of α lath as shown in Figure 2(d). The different microstructures between the Ti alloys treated at 800 °C and 900 °C can be attributed to α/β transformation at 847 °C. The grain size distributions of the Ti alloys under different conditions are plotted in Figure 3. It should be noted that the grain size for equiaxed α/β grains and $\beta+\alpha$ colonies were measured as grain diameter and colony size, respectively. Statistical results were collected from overall microstructures for each condition by applying intercept method for grain diameter and area calculation for frequency [8, 9]. It shows that after solution treatments at high temperatures of 800 °C and 900 °C, the peak diameter of α/β grains increases from 1 μm to 2.5 μm and 3 μm , respectively. In addition, the peak diameter of $\beta+\alpha$ colonies increases from 2.5 μm to about 4 μm after corresponding aging treatments.

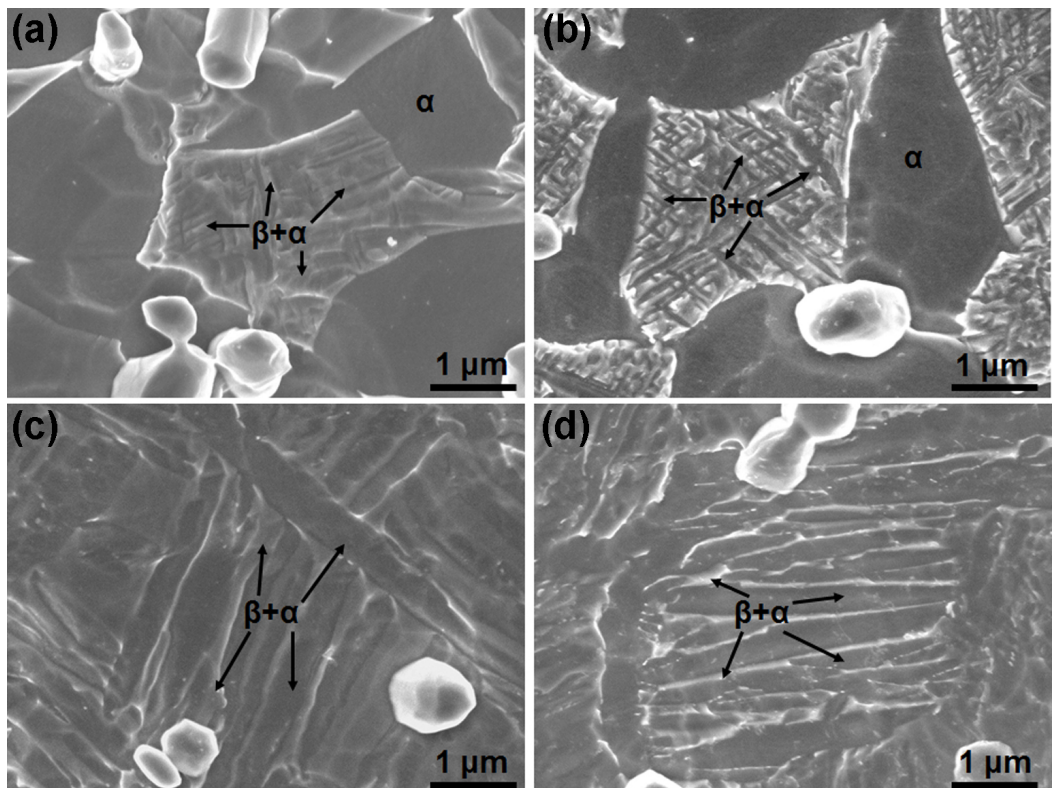


Figure 2. SEM observations of Ti alloys after different heat treatments: (a) 800 °C; (b) 800 °C+500 °C; (c) 900 °C; (d) 900 °C+500 °C.

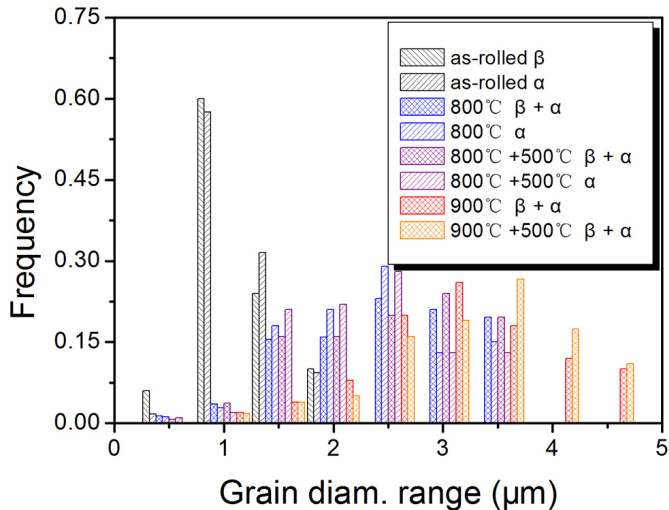


Figure 3. Grain diameter distributions of the Ti alloys under different conditions.

Figure 4(a) shows clean particle with a diameter of about 1 μm indexed as $(\text{TiHf})_5\text{Si}_3$ as shown in inset. It should be noted that $(\text{TiHf})_5\text{Si}_3$ has same crystal structure as Ti_5Si_3 with partial Hf atoms occupation instead of Ti atoms in unit, and the detail of $(\text{TiHf})_5\text{Si}_3$ formation has been reported in our previous work [8]. Figure 4(b) shows high density dislocations generated near $(\text{TiHf})_5\text{Si}_3$ particle, indicating pinning effect of particle-reinforcement on dislocation motion.

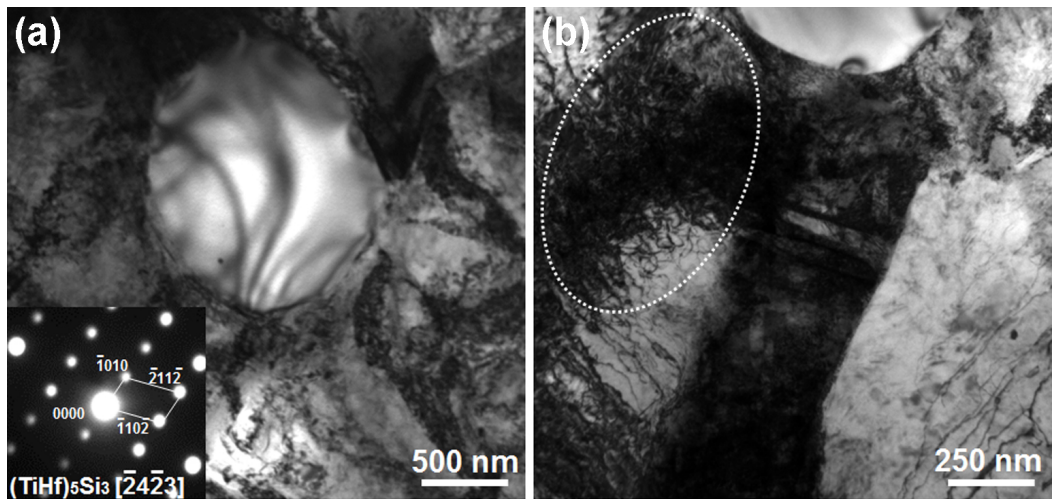


Figure 4. TEM observations of as-rolled Ti alloy: (a) $(\text{TiHf})_5\text{Si}_3$ particle embedded in Ti matrix with inset showing the diffraction pattern of $(\text{TiHf})_5\text{Si}_3$; (b) high density dislocations marked by dash ellipse close to $(\text{TiHf})_5\text{Si}_3$ particle.

3.2 Tensile behavior

Figure 5 shows tensile engineering stress-strain curves of the Ti alloys under different conditions. In general, the Ti alloys reveal good combination of strength and ductility. The as-rolled Ti alloy presents highest ultimate tensile strength of 950 MPa with a total elongation of 12%. With increasing solution treatment temperature and corresponding aging treatment, the ultimate tensile strength of the Ti alloys decreases gradually from 900 MPa to 865 MPa with slightly increment of elongation from 12% to 14%.

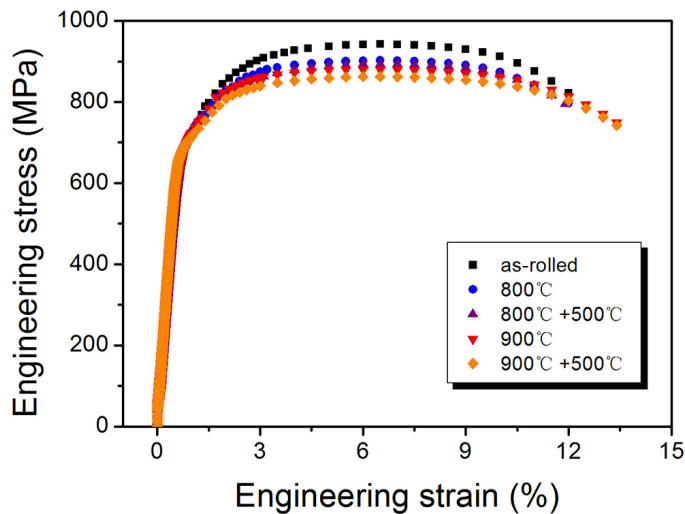


Figure 5. Tensile engineering stress-strain curves of the Ti alloys under different conditions.

4. Discussion

With uniform distribution of particle reinforcements, the strengthening of the Ti alloy can be attributed to i) particle strengthening, ii) solid-solution strengthening, iii) grain boundary strengthening and iv) dislocation strengthening.

4.1 Particle strengthening

The novel Ti alloy is reinforced by $(\text{TiHf})_5\text{Si}_3$ particles and the average diameter of these particles can be kept as about 1 μm even after high temperature heat treatment for a long period as shown in Figure 1 and 2. Moreover, the existence of $(\text{TiHf})_5\text{Si}_3$ particles located at grain boundaries and triple junctions can resist the growth of matrix Ti grains. Particle strengthening performs in two ways. On the one hand, the $(\text{TiHf})_5\text{Si}_3$ particle itself has higher module and sustains higher stress theoretically at equivalent strain than Ti

matrix. On the other hand, the $(\text{TiHf})_5\text{Si}_3$ particles can hinder the dislocation motion and thereafter cause dislocations accumulations close to $(\text{TiHf})_5\text{Si}_3$ particles.

4.2 Solid-solution strengthening

Solid-solution strengthening can be caused by alloyed elements with different atom size compared to metal matrix due to unit misfit and relative variation of strain fields. Local strain fields can be created and interact with dislocations for example impede their motion, leading to increasing strength. Si added in this Ti alloy partially forms $\text{Ti}(\text{Si})$ solid solution with very low Si concentration [10] and forms silicide at the same time. Nb, Fe, Ta and W act as solid-solution elements in the Ti matrix. Hf also may act as solid-solution element in the Ti matrix and is likely to solute in the Ti_5Si_3 phase resulting in the $(\text{TiHf})_5\text{Si}_3$ compound phase [8].

4.3 Grain boundary strengthening

According to the Hall-Petch relationship, the yield strength of Ti increases with decreasing grain size. The average grain diameter d of the Ti alloy under different conditions can be calculated by expectation according to statistical results from Figure 3. The stress-grain size relationship at a strain of 2% with a dash drawn line by idealized modeling is given as shown in Figure 6 and it turns out that the strength of the Ti follows the Hall-Petch relationship well. It should be noted that, the given strain is 2% since the grain size of the Ti alloy is generally small and therefore notable response of dislocation slip demands higher strength instead of yield strength at a strain of 0.2%. In addition, a misfit strain may be created due to mismatch deformation behavior between α and β phase during tension thereafter be relaxed by formation of geometrically necessary dislocations (GND) near phase boundaries [11]. The phase boundaries in this way can also strengthen the Ti alloys to some extent.

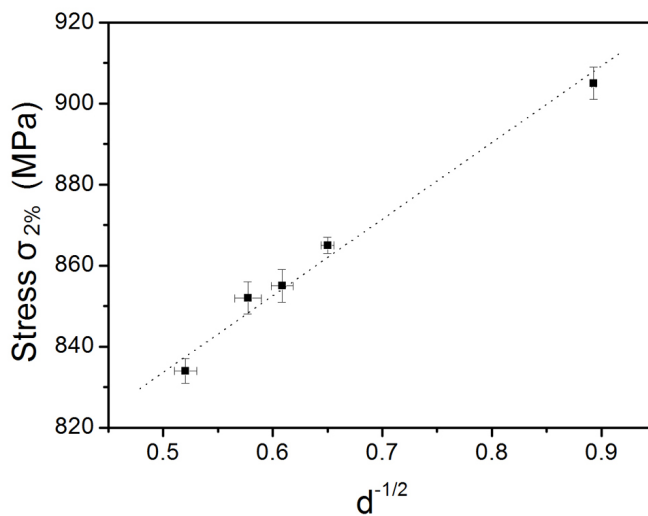


Figure 6. The stress-grain size relationship at a strain of 2% with a dash drawn line by idealized modeling.

4.4 Dislocation strengthening

The difference in thermal expansion between $(\text{TiHf})_5\text{Si}_3$ particle and Ti matrix may give rise to a thermal stress at interface between them during air cooling after heat treatments. This may cause elastic/plastic deformation near the interface to some extent leading to dislocations generated near the $(\text{TiHf})_5\text{Si}_3$ particles (Figure 4(a)). The dislocation density ρ caused by residual thermal stress can be calculated according to ref [12] as:

$$\rho = \frac{B f \Delta\alpha \Delta T R}{b(1-f)D}$$

where B is a geometric constant, b is the Burger's vector of the Ti matrix, $\Delta\alpha$ is the difference of thermal expansion coefficients between $(\text{TiHf})_5\text{Si}_3$ particle and Ti matrix, ΔT is temperature variation, and f , R , and D are the volume fraction, aspect ratio and diameter of the particles, respectively. Moreover, the different elastic/plastic properties between $(\text{TiHf})_5\text{Si}_3$ particle and Ti matrix may cause mismatch in strained Ti alloy leading to the GND formation near the interface. These dislocations resulted from thermo mismatch and mechanical mismatch between the $(\text{TiHf})_5\text{Si}_3$ particle and the Ti matrix may creat extra strengthening effect on the Ti alloy.

5. Conclusions

A novel Ti-2Si-2Nb-2Fe-1Hf-1Ta-1W alloy with $(\text{TiHf})_5\text{Si}_3$ particle-reinforcement has been fabricated, exhibiting good mechanical performance. The $(\text{TiHf})_5\text{Si}_3$ particles can be kept as about 1 μm even after high temperature heat treatment for a long period. With uniform distribution of the $(\text{TiHf})_5\text{Si}_3$ particle-reinforcement at grain boundaries and triple junctions, multiple strengthening mechanisms have been found including i) particle strengthening, ii) solid-solution strengthening, iii) grain boundary strengthening and iv) dislocation strengthening.

6. Acknowledgements

The authors gratefully acknowledge the support from the National Natural Science Foundation of China (Grant No. 51701163 and U1737108), within which part of this work was performed.

7. References

- [1] K. Wang, Mater. Sci. Eng. A 213 (1996) 134-137.
- [2] R.R. Boyer, Mater. Sci. Eng. A 213 (1996) 103-114.
- [3] Y.F. Yang, S.D. Luo, C.J. Bettles, et al, Mater. Sci. Eng. A 528 (2011) 7381-7387.
- [4] Z. Hu, Y. Zhan, J. She, Mater. Sci. Eng. A 560 (2013) 583-588.

- [5] X. Zhang, M. He, W. Yang, et al, Mater. Sci. Eng. A 698 (2017) 73-79..
- [6] S. Abdi, M.S. Khoshkho, O. Shuleshova, et al, Intermetallics 46 (2014) 156-163.
- [7] X. Ma, X. Guo, M. Fu, et al, Mater. Char. 142 (2018) 332-339.
- [8] J. Lu, Y. Zhao, Y. Du, et al, J. Alloy. Compd. 778 (2019) 115-123.
- [9] G.M. Le, A. Godfrey, N. Hansen, Mater. Des. 49 (2013) 360-367.
- [10] J.L. Murray, ASM Int. (1987) 289-293.
- [11] M.F. Ashby, Philos. Mag. 21 (1970) 399-424.
- [12] R.J. Arsenault, N. Shi, Mater. Sci. Eng. A 81 (1986) 175-187.